Original Article The Eurasian Journal of Medicine Eurasian J Med 2013; 45: 115-25

An Analysis of the Anatomic Variations of the Paranasal Sinuses and Ethmoid Roof Using Computed Tomography

Paranasal Sinüsler ve Etmoid Çatının Anatomik Varyasyonlarının Bilgisayarlı Tomografi ile Analizi

Hatice Kaplanoglu[1], Veysel Kaplanoglu[2], Alper Dilli[1], Ugur Toprak[2], Baki Hekimoğlu[1]

[1]Department of Radiology, Diskapi Yildirim Beyazit Training and Research Hospital, Ankara, Turkey

[2]Department of Radiology, Ankara Numune Training and Research Hospital, Ankara, Turkey

Abstract

Objective: To determine the Keros classification and asymmetrical distribution rates of the ethmoid roof and the frequency of anatomic variations of the paranasal sinuses.

Materials and Methods: Paranasal sinus scans of 500 patients obtained using computed tomography were evaluated retrospectively. Measurements were performed using a coronal plan with right-left comparison and with distance measurement techniques. The depth of the lateral lamella was calculated by subtracting the depth of the cribriform plate from the depth of the medial ethmoid roof. The results were classified according to their Keros classification. Any asymmetries in the ethmoid roof depth and fovea ethmoidalis configuration were examined. The anatomic variations frequently encountered in paranasal sinuses (pneumatized middle concha, paradoxical middle concha, agger nasi cells, Haller cells, Onodi cells, etc.) were defined.

Results: The mean height of the lateral lamella cribriform plate (LLCP) was 4.92±1.70 mm. The cases were classified as 13.4% Keros Type I, 76.1% Keros Type II, and 10.5% Keros Type III. There was asymmetry in the LLCP depths of 80% of the cases, and a configuration asymmetry in the fovea in 35% of the cases. In 32% of the cases with fovea configuration asymmetry, there was also asymmetry in the height of the right and left LLCP. The most frequent variations were nasal septum deviation (81.8%), agger nasi cells (63.8%), intralamellar air cells (45%), and concha bullosa (30%).

Conclusion: Using the Keros classification for LLCP height, higher rates of Keros Type I were found in other studies than in our study. The most frequent classification was Keros Type II. The paranasal sinus variations in each patient should be carefully evaluated. The data obtained from these evaluations can prevent probable complications by informing rhinologists performing endoscopic sinus surgery about preoperative and intraoperative processes.

Key Words: Anatomic variations, asymmetric dispersion of ethmoid roof depth, ethmoid roof, keros classification, paranasal sinus

Özet

Amaç: Etmoid çatının Keros klasifikasyonu, asimetrik dağılım oranları ve paranazal sinüslerin anatomik varyasyonlarının sıklığının belirlenmesidir.

Gereç ve Yöntem: Bilgisayarlı tomografisi incelemesi ile 500 olgunun paranasal sinüslerinin görüntüleri retrospektif olarak değerlendirildi. Ölçümler koronal planda, sağ-sol karşılaştırmalı ve mesafe ölçüm tekniği ile yapıldı. Medial etmoid tavan yüksekliğinden kribriform plate yüksekliği çıkarılarak lateral lamella yüksekliği hesaplandı. Sonuçlar Keros klasifikasyonuna göre sınıflandırıldı. Etmoid tavan yükseklik asimetrisi ve fovea etmoidalis şekil asimetrisi araştırıldı. Paranazal sinüslerde sık karşılaşılan anatomik varyasyonlar (pnömotize orta konka, paradoksal orta konka, Agger nasi hücresi, Haller hücresi, Onodi hücresi, supraorbital hücre, anteriyor klinoid proçes ve unsinat proçes havalanması, maksiler sinüs varyasyonları) tanımlandı.

Bulgular: Kribriform plate lateral lamella (LLKP)'nın ortalama yüksekliği 4.92±1.70 mm idi. Olguların %13.4' ü Keros Tip I, %76.1'i Keros Tip II ve %10.5'i Keros Tip III olarak sınıflandırıldı. Olguların %80'inde LLKP yüksekliklerinde asimetri, %35'inde foveada şekil asimetrisi saptandı. Fovea şekil asimetrisi olan olguların %32'sinde sağ ve sol LLKP yüksekliklerinde de asimetri vardı. En sık nasal septum deviasyonu (%81.8), Agger nasi hücresi (%63.8), intralameller hava hücresi (%45) ve konka bulloza (%30) varyasyonları saptandı.

Sonuç: LLKP yüksekliği Keros' a göre sınıflandırıldığında, diğer çalışmalarda Keros Tip I daha fazla oranda izlenirken, bizde çok daha az oranda izlendi. En sık Keros tip II bulundu. Her olgunun paranazal sinüsleri varyasyon açısından dikkatle değerlendirilmelidir. Elde edilen veriler, endoskopik sinüs cerrahisi için rinologlara preoperatif ve intraoperatif süreçlerde yol göstererek olası komplikasyonların oluşumunu engeller.

Anahtar Kelimeler: Anatomik varyasyonlar, etmoid çatı, etmoid çatı yüksekliğinin asimetrik dağılımı, keros klasifikasyonu, paranasal sinus

Received: November 29, 2012 / **Accepted:** March 02, 2013

Correspondence to: Hatice Kaplanoglu, Department of Radiology, Diskapi Yildirim Beyazit Training and Research Hospital, TR-06100 Ankara, Turkey
Phone: +90 312 508 44 43 e-mail: hatice.altnkaynak@yahoo.com.tr

doi:10.5152/eajm.2013.23

Introduction

Currently, endoscopic sinus surgery (ESS) is extensively utilized. It is used not only for the treatment of chronic rhinosinusitis that is resistant to medical treatment but also in the treatment of a number of diseases such as nasal polyposis, mucocele, sellar and parasellar tumors, and optic nerve decompression [1]. There may be complications to endoscopic sinus surgery because it is performed in a complex region. These complications are divided into categories minor and major complications. Minor complications occur in 1.1%-20.8% of the cases in which ESS is performed. These complications are hemorrhage, infection, cohesion, obstruction/narrowness in the ostium, topognosis/insensitivity the in teeth or lips, and the relapse of the disease. The major complications are cerebrospinal fluid leakage, ocular traumatization, meningitis or intracranial vascular traumatization; these complications occur in 0-1.5% of cases [2-4]. To minimize probable complications and to avoid major complications, anatomic variations, particularly in the base of the skull, should be properly understood.

The majority of the major complications are related to the ethmoid bone. The most complex and variable structure of the paranasal sinuses is the ethmoid sinus. The fovea ethmoidalis makes up the roof of the ethmoid bone labyrinth. The fovea ethmoidalis is a part of the frontal bone that separates the ethmoidal cells from the anterior cranial fossa. The fovea ethmoidalis also medially connects with the lateral lamella of the cribriform plate (Figure 1). The lateral lamella is the thinnest/finest and most vulnerable bone of the skull base [5, 6]. The fovea ethmoidalis and lateral lamella are the most important parts of the skull base in terms of the risk of complication development during ESS [7, 8].

Keros classified the depth of the olfactory fossa into 3 types based on the height of the lateral lamella [5]. The depth of the olfactory fossa is 1-3 mm in Type I, 4-7 mm in Type II, and 8-16 mm in Type III. According to Keros, the greater the height of the lateral lamella, the higher the risk of its penetration into the anterior cranial fossa [9].

The presence or absence of asymmetry in the paranasal sinuses can be determined. Asymmetry in the anterior of the skull base and especially in the ethmoid roof is important for ESS. If asymmetry is present, the height of the ethmoid roof varies, and the fovea ethmoidalis of the two sides may be at different levels [10, 11]. Similarly, the presence or absence of a variation in the contour of one side of the fovea can also be determined. The shape of the contour of the fovea is determined by the angle at which the fovea ethmoidalis joins with the cribriform plate. The fovea ethmoidalis may be straight or in the shape of a broken wing if the joint angle increases [11]. Intracranial complications appear more frequently on the side in which the ethmoid roof is low. This low-hanging roof may cause cerebrospinal fluid fistula and recurrent meningitis postoperatively [10, 11].

An understanding of the anatomy, diseases, and variations of the paranasal sinus has become possible with the development and proliferation of computed tomography (CT). Understanding the paranasal sinus anatomy for each patient has been a directive in sinus surgery, which in turn enables complication avoidance.

We performed a Keros classification of the ethmoid roof, determined the asymmetrical distribution ratios, and investi-

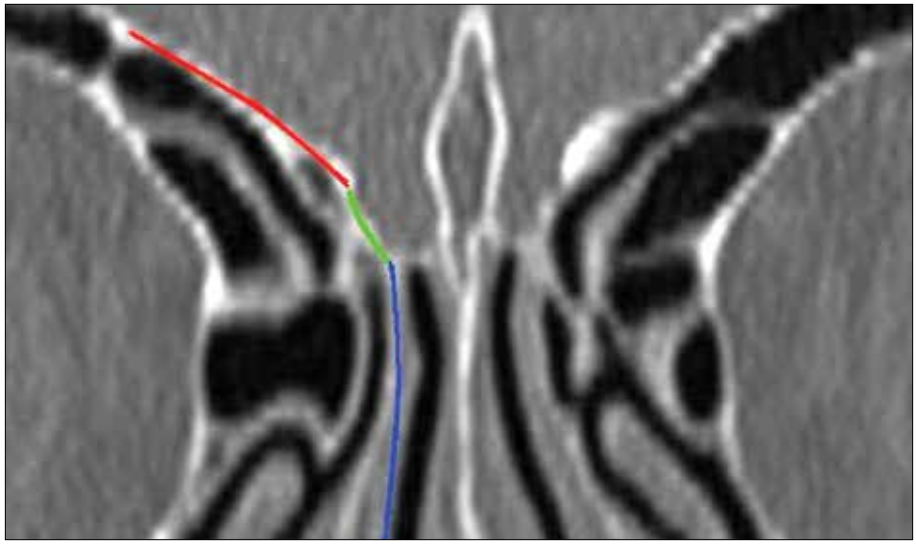

Figure 1. *Paranasal coronal tomography cross-section. Red: fovea ethmoidalis; blue: cribriform plate; green: lateral lamella.*

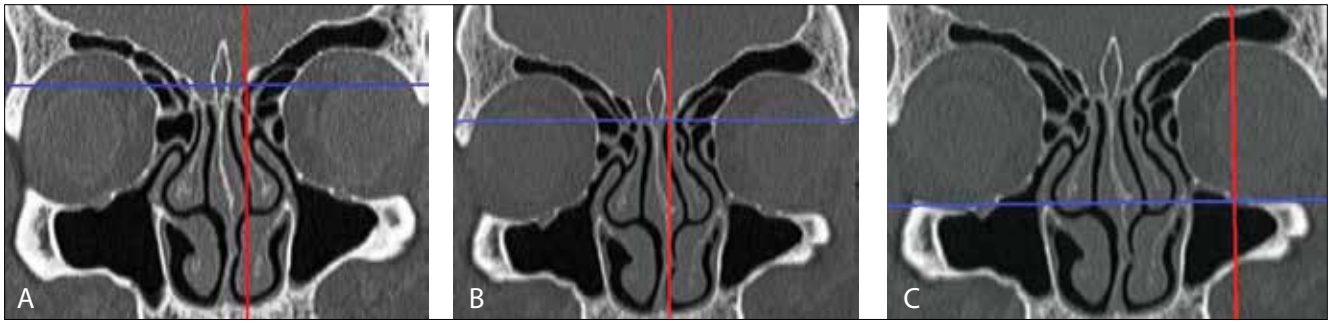

Figure 2. *A) In a coronal paranasal sinus CT cross-section, the point where the ethmoid roof medially intersects with the lateral lamella, B) cribriform plate point, C) infraorbital nerve point.*

gated the frequency of the anatomic variations of the paranasal sinuses to further understand the anatomy of the skull base. The end goal of these investigations was to gather this knowledge in an effort to reduce the rate of complications of endoscopic sinus surgery.

Materials and Methods

Images obtained from 500 patients who underwent paranasal sinus CT for various reasons at our hospital between January 2011 and December 2011 were evaluated retrospectively. The study excluded patients who sustained skull base fractures, sinonasal tumors, nasal polyposis, skull base or sinus surgery, serious rhinosinusitis and individuals who are below the age of 18. Examinations were performed using tomography equipment (Philips Marconi MX8000, Royal Philips Electronics, Amsterdam, The Netherlands) with 4 detectors. As shooting parameters, 120 kVp; 120-150 mAs; 200 mm FOV and a pitch of 1.75 were utilized. All shootings were performed on a coronal plane in a perpendicular projection from the hard palate with a 2.5 mm cross-section thickness and a 3 mm cross-section pitch. Computed tomography images were analyzed using MX-View software, version 3.52. The images were examined in the bone window on a digital screen. All of the cases included in the study were evaluated by the same radiology expert. The ethmoid roof measurements were performed manually using a digital screen. Standard anatomic points [2] were determined and used during the measurements. These points were the medial ethmoid roof (the point where the ethmoid roof medially joins with the lateral lamella (Figure 2a)), the cribriform plate point (Figure 2b), and the infraorbital nerve point (Figure 2c). Measurements were performed using the distance measurement technique in the coronal plane. A horizontal plane was established by crossing the horizontal line with the infraorbital nerves. The length of the vertical line drawn from the medial ethmoid roof to the horizontal plane was defined as the medial ethmoid roof height. The length of a vertical line drawn from the cribriform plate to the horizontal plane was defined as the cribriform plate height (Figure 3). The height of the lateral lamella was calculated by subtracting the cribriform height from the medial ethmoid roof height [12]. Measurements between the right and left sides were compared. The results were categorized according to Keros classification, and their distributions were analyzed according to gender.

The configuration formation was measured from the point at which the fovea ethmoidalis joins with the lateral lamella. This formation was evaluated as having either a straight or broken wing configuration, and asymmetry in the configuration was investigated. The depth of the ethmoid roof was divided into 3 categories: a) symmetrical right and left roof depth, b) right ethmoid roof depth lower than the left, and c) left ethmoid roof depth lower than the right.

Because the anatomy of the drainage pathways and anatomic variations in paranasal sinuses are directive in ESS, these were also investigated. Variations for each case, as defined below, were scored as present or absent, and their distribution between genders was analyzed. These variations were:

1. Pneumatized middle concha: the pneumatization of the inferior bullous part or the vertical lamellar part (the part that remains above the osteomeatal complex) of the middle concha. This is generally bilateral and its prevalence is 24-55%. Pneumatization of both vertical lamellas and inferior bullous parts were accepted as concha bullosa [13].
2. Paradox middle concha: the middle concha convexity is positioned toward the lateral end. This is found in approximately 26% of the population [13]. The presence of paradox concha was accepted when the paradox curvature was observed in at least 2 consecutive cross-sections [14].
3. Agger nasi cell: the anterior ethmoidal air cell below the frontal sinus. In CT examination, the paranasal sinus is found in coronal cross-sections at the anterior region of the joint connecting the middle concha to the skull

base. This structure makes up the anterior and inferior wall of the recess [13].

4. Haller cell (infraorbital ethmoidal cell): localized at the inferior of the ethmoid bulla. The Haller cell is an air cell formed on the maxillary sinus medial roof with the pneumatization of the orbital inferomedial wall [13, 14].
5. Onodi (sphenoethmoidal) cell: formed as a result of the posterior ethmoid air cell stretching towards the superior and lateral sphenoid sinus. This structure is localized between the skull base and the sphenoid sinus. It pushes the sphenoid sinus inferiorly [13].
6. Supraorbital cell: formed as a result of the anterior ethmoidal cell stretching towards the frontal sinus orbital plate, frontal sinus, and its superior. The supraorbital cell is generally bilateral [13].
7. Maxillary sinus variations: Maxillary sinus (MS) variations include sinus septation, accessory ostium, and sinus hypoplasia. Maxillary sinus septa may be fibrous or bone and generally stretch from the infraorbital canal to the lateral wall. Accessory ostium is localized at the posterior of the natural ostium and is found in 10% of the population [13]. There are 3 types of maxillary sinus hypoplasia. In type I, there is a slight hypoplasia and a normal uncinate process. In type II, there is a serious hypoplasia and an abnormal uncinate process. In type III, there is a fissured antrum in and no uncinate process [14].
8. Uncinate process pneumatization: the uncinate process lies along the anterior and superior of the frontal recess and along the inferior of the lower concha. Uncinate process pneumatization was detected in this study [13].
9. Anterior clinoid process pneumatization: an anterior clinoid process surrounds the optic nerve. This is found in 6-13% of cases [13].

Statistical Analysis

SPSS 17.0 was utilized for the statistical analysis. The data obtained was evaluated using the descriptive statistical methods (mean, standard deviation, median, frequency). The Mann Whitney U test was also performed to determine which group had the largest variation and to evaluate the two groups. The difference between the means of the continuous variables according to gender was tested using an unbiased sample t-test. The difference between the means of the two paired groups was evaluated using the paired sample t-test. The chi-square test was used to compare the qualitative data. Spearman's correlation analysis was used to evaluate the relationship between the parameters. The results were evaluated in a 95% validity range, and $p<0.05$ was considered significant.

Results

CT scans of the 500 cases were analyzed. Of these cases, 261 (52.2%) were female and 239 (47.8%) were male. The average age of the patients was 39.41 with a median value of 38 (18-81). The average age of the females was 38.90, and the average age of the males was 39.94. The average height of the lateral lamella cribriform plate (LLCP) was 4.92±1.70 mm, and the median was 4.90 (0.9-10.5). The average height of the LLCP was 4.87±1.71 mm for the right side and 4.91±1.66 mm for the left side. The average difference between the right and left LLCP heights was 0.090±0.96 mm, which is statistically significant ($p=0.036$). The average height of the LLCP was found to be lower on the right side.

There was no difference between the genders regarding right and left LLCP height ($p>0.05$). In females, no difference was found between the right and left LLCP height ($p=0.403$); in males, the LLCP height was higher on the left side than the right side ($p=0.045$) (Table 1). When the right and left LLCP heights were compared for each individual, asymmetry (a height difference between two sides>1 mm) was found in 400 cases (80%) (Figure 4). A lower left side LLCP height was found in 184 cases (46%), and a lower right side LLCP height was found in 216 cases (54%) (Table 2). When the right and left LLCP heights of the 500 cases were examined, the difference between the right and left LLCP heights was >2 mm in ten (2%) cases (four female, six male). The distribution of the differences between the right and left LLCP heights according to gender are presented in Table 3.

According to Keros classification, the LLCP height complies with Keros Type I in 134 (13.4%) sides, Keros Type II in 761 (76.1%) sides, and Keros Type III in 105 (10.5%) sides (Figure 5, Table 4). The average LLCP height was 3.21±1.72 mm in Keros Type I cases, 4.85±1.29 mm in Keros type II cases, and 7.54±0.89 mm in Keros Type III cases. The right and left sides were classified as having different Keros types in 5.04% of the male cases and 6.87% of the female cases (Table 5). No significant differences were found between the female and male cases in terms of the distribution of Keros classification types ($p>0.05$).

Table 1. Cribriform plate lateral lamella depth (mm)±Standard deviation

Cribriform plate lateral lamella depth (mm)±Standard deviation			
	Right	Left	Overall
Female	4.78±1.63	4.84±1.63	4.77±4.80
Male	4.98±1.80	5.11±1.68	4.99±5.05
Overall	4.87±1.71	4.91±1.66	4.92±1.70

Table 2. Distribution and percentage values of the cribriform plate lateral lamella depth according to Keros classification

Keros Type	Right		Left		Overall
	Male	Female	Male	Female	
Type I (0-3 mm)	26 (10.9)	42 (16)	25(10.5)	41 (15.6)	134 (13.4)
Type II (3.1-7 mm)	183 (76.9)	198 (75.6)	184 (48.4)	196 (51.6)	761 (76.1)
Type III (>7 mm)	29 (12.2)	22 (8.4)	29 (12.2)	25 (9.5)	105 (10.5)
Overall	238 (100)	262 (100)	238 (100)	262 (100)	1000 (100)
N (%) given					

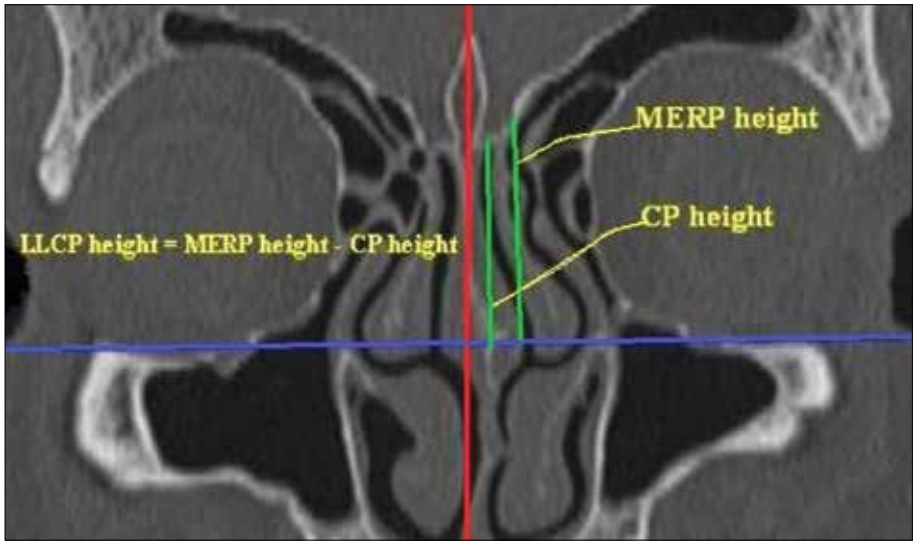

Figure 3. *Measurement of the depth of the lateral lamella in a coronal paranasal sinus CT cross-section.*

There was no statistically significant difference between female and male cases in terms of the frequency of a low ethmoid roof or the symmetry-asymmetry ratios (p>0.05).

Configuration asymmetry in the fovea was found in 175 cases (35%). Configuration asymmetry in the fovea was bilateral in ten cases and one-sided in 160 cases. There was asymmetry between the right and left LLCP heights in 160 (32%) of the cases with configuration asymmetry in the fovea. Fovea configuration asymmetry was present in only nine cases. Of these, eight had configuration asymmetry in the left fovea and one had it in the right fovea (Table 6).

Configuration asymmetry in the fovea was found more frequently in the left side than the right side. When the distribution of the right and left fovea configuration asymmetry was examined according to gender, configuration asymmetry in both the right and left sides was more prevalent in males than in females. The distribution of fovea asymmetry, between gender and right/left sides, was p=0.04 for the right side and p=0.014 for the left side. This difference was statistically significant.

Anatomic variations frequently found in the paranasal sinus region and the distribution of anatomic variations according to gender are shown in Table 7. Right anterior clinoid pneumatization was found more frequently in males (p=0.014), and MS hypoplasia and bone septum in the MS were more prevalent in females (p=0.001). There was no statistically significant difference between genders for the other variations.

Discussion

The frontal bone of the ethmoid roof region is thick and dense. The thicker frontal bone is medially placed near the thinner lateral lamella of the ethmoid bone [15]. The lamina lateralis of the lamina cribrosa forms the thin medial wall of the ethmoid roof. The intracranial traumatization risk is the

Table 3. Cribriform plate lateral lamella depth values according to Keros classification

Approximate cribriform plate lateral lamella depths (mm)			
	Type I	Type II	Type III
Right Side	2.30	4.91	8.00
Left Side	2.36	4.89	7.75
Overall	3.21	4.85	7.54

highest in the lateral lamella of the lamina cribrosa during ESC because it is the thinnest part of the ethmoid roof. A long segment of the lateral lamella can be found in cases with a deep cribriform plate. Paranasal sinus CT scans obtained only in the coronal plane can provide adequate information regarding the individual variations and ethmoid roof depths of patients [15].

With advances in endoscopic sinus surgery, CT examination has become a part of preoperative evaluation. Together with the clinical examination and nasal endoscopy in the preoperative period, CT scans are necessary for determining the pathological changes and anatomic variations of a given set of nasal and paranasal sinuses. The lateral lamella, a thin bone component of the lamina cribrosa, forms the medial wall of the ethmoid roof. The thickness of the lamina cribrosa is between 0.05-0.2 mm. Using radiological means to determine the length and width of the olfactory fossa, as well as the depth of the ethmoid roof are crucial for planning the upper limit of the dissection. Without radiological scans, anterior cranial fossa penetration and resulting cerebral damage, hemorrhage, and BOS fistula are probable complications that can occur during the operation or in the postoperative period [3, 4]. CT examinations should be used to explore the paranasal sinuses in the preoperative period because they provide a map for the surgical procedure and assist in complication avoidance. To our knowledge, there has been no other study that has investigated the depth and asymmetry of the ethmoid roof and paranasal sinus variations in female and male using such a large sample in Turkey. In this study, a specially designed work station and computed tomography with a multiplanar reconstruction were used to investigate anatomic variations and ethmoid roof depth and asymmetry in detail.

Figure 4. *In a coronal paranasal sinus CT cross-section, A) Type I, B) Type II, C) and Type III lateral lamella depths according to Keros classification.*

Table 4. Distribution and percentage values of the right and left cribriform plate lateral lamella depth differences according to gender

		Female		Male	
	(mm)	n	%	n	%
Depth Difference	<1	235	89.7	210	88.2
	1-2	23	8.8	22	9.3
	>2	4	1.5	6	2.5
	Toplam	262	100,0	238	100,0

Figure 5. *Asymmetrical ethmoid roof in a coronal paranasal sinus CT cross-section.*

Table 5. Distribution and percentage values of the cribriform plate lateral lamella depth in symmetry-asymmetry (low ethmoid roof) groups

	Female n (%)	Male n (%)	Total n (%)
Right ethmoid roof low	113 (43.1)	103(43.3)	216 (43.2)
Left ethmoid roof low	98 (37.40)	86 (36.1)	184 (36.8)
Total asymmetry (right or left ethmoid roof low)	211 (80.5)	189 (79.4)	400 (80)
Symmetry	51 (19.5)	49 (20.6)	100 (20)
Overall (symmetry+ asymmetry)	262 (100)	238 (100)	500 (100)

In his anatomical study, Keros analyzed the ethmoid roof of 450 skulls. Keros created three categories for the classification of the olfactory groove according to LLCP height. Type I (1-3 mm) was found in 12% of the specimens, Type II (4-7 mm) in 70% of the specimens, and Type III in 18% of the specimens [16]. There have been analyses on the ethmoid roof in a variety of ethnic groups. Alazzawi et al. [12] analyzed the ethmoid roof in 3 ethnic groups (150 cases from Malaysia, China, and India) and classified 80% of the cases as Keros Type I and 20% of the cases as Keros Type II. They did not find any that were Keros Type III. They found that Keros Type II was more prevalent in men than in women ($p<0.001$) [2]. In a study with 300 adult cases, Elwany et al. [17] from Egypt classified 42.5% of the cases as Keros Type I and 56.8% of the cases as Keros Type II. Keros Type III was found in 1.4% of the men and in none of the women. Elwany et al. [19] reported that Keros Type II was found more frequently in men, and Keros Type I was found more frequently in women. Souza et al. [18] from Brazil evaluated the CT scans of 200 cases and found that Keros Type II was the most frequent type (73.3%) followed by Type I (26.3%) and Type III (0.5 %). Solares et al. [19] evaluated 50 CT scans in the United States. They found that 83% of the cases were Keros Type I, 15% were Type II, and 2% were Type III. These studies support and strengthen the hypothesis that the ethmoid roof configuration varies between populations.

In their ethmoid roof analysis of 136 cases, Erdem et al. [20] found that 8.1% of the cases were Keros Type I, 59.6% were Keros Type II, and 32.3% were Keros Type III. Şahin et al. [21] examined 100 paranasal sinus CT scans in their study and reported that 10% of the cases were Keros Type I, 61% were Keros Type II, and 29% were Keros Type III. In the study presented here, of the 1,000 total examinations (two sides in each patient), 13.4% were Keros Type I, 76.1% were Keros Type II, and 10.5% were Keros Type III. Type I was more prevalent in women than men (31.6%/21.4%), and Type III

Table 6. Distribution and percentage values of fovea configuration asymmetry according to gender

	Right fovea configuration asymmetry	Left fovea configuration asymmetry	Total
Female	28 (10.7)	41(15.7)	69 (39.4)
Male	48 (20.1)	58 (25.3)	106 (60.6)
Total	76	99	175 (100)
N(%)given			

was more prevalent in men than women (24.4%/17.9%). The results of our study are compatible with the study results of Keros, and there is no significant difference between the rates found in our study and the rates found in his.

The differences between the results of this study and the other studies conducted on Turkish populations may be due to the use of different measurement techniques. The cross-section in which the infra-orbital nerve follows the base of the orbita was taken as the reference point for the measurements in this study. Literature has reported that this reference point is more relevant during surgery, can be identified after endoscopic maxillary antrostomy, and can assist in informing the surgeons of the position of the ethmoid roof, especially for cases in which endoscopic maxillary sinus antrostomy is performed [19].

Meloni et al. determined the depth of the cribriform plate to be 5.9 mm on average (range 1.3-17 mm) in subjects from Italy [22]. Alazzawi et al. [12] found a mean (SD) height of 2.64 mm (1.45 mm) for the LLCP in their study on 3 ethnic groups in Malaysia. Regarding the studies conducted on the Turkish population, Aslan et al. [23] found a mean of 8 mm (range 2-14 mm) for the height of the right side of the ethmoid roof, and a mean of 9.5 mm (range 3-16 mm) for the height of the left side. Erdem et al. [20] found a mean height of 6.1±2.2 mm of the ethmoid roof on the right side and a mean of 6.1± 2.3 mm for the left side. Şahin et al. [21] found a 6 mm average ethmoid roof height on the left side and a 6.2 mm average height on the right side. In the study presented here, the mean (SD) height of the LLCP in 1,000 total sides of the ethmoid roof was 4.92±1.70 mm. The mean height of the right side of the ethmoid roof was 4.87±1.71 mm, and the mean height of the left side was 4.91±1.66 mm. We found approximately 0.090±0.96 mm difference between the right and left LLCP heights.

A number of studies report a lower ethmoid roof mean height on the right side than on the left side [9, 17, 22, 24-26]. In their study conducted on a Turkish population, Arikan et al. [27] determined that their subjects had a higher left side ethmoid roof than right side ethmoid roof. In this study, LLCP height was found to be lower on the right side than on the left side, and there was a significant difference between the right and left LLCP heights ($p = 0.036$).

Table 7. Distribution and percentage values of the anatomic variations according to gender

	Gender				Total	
	Female		Male			
	n (262)	%	n (238)	%	n (500)	%
Concha bullosa	75	28.6	77	32.3	152	30.4
Intralamellar Air Cell	124	47.5	101	42.3	225	45
Paradoxal middle concha	42	16.1	31	13	73	14.6
Pneumatized agger nasi	168	64.4	151	63.2	319	63.8
Haller cell	43	16.5	32	13.4	75	15
Onodi cell	26	10	27	11.3	53	10.6
Supraorbital Air Cell	14	5.4	17	7.1	31	6.2
Nasal septum deviation	213	81.6	196	82	409	81.8
Spur formation	135	51.7	120	50.2	255	51
Left ant. clinoid pneumatization	58	22.2	61	25.5	119	23.8
Right ant. clinoid pneumatization	48	18.4	66	27.6	114	22.8
Accessory ostium in MS	43	16.4	39	16.4	82	16.4
MS hypoplasia	4	1.5	0	0	4	0.8
Bone septum in MS	26	10	36	15.1	62	12.4
Unsinat process pneumatization	9	3.5	10	4.2	19	3.8

Table 8. Distribution of the paranasal sinus anatomic variations according to their rates in paranasal sinus CT studies in different countries

	n	Concha Bullosa (%)	Paradoxal Middle Concha (%)	Agger Nasi Cell (%)	Haller Cell (%)	Onodi Cell (%)
Study presented (country)	500	30.4	14.6	63.8	15	10.6
Arslan (22) (Turkey)	200	30	—	—	6	12
Kantarcı (32) (Turkey)	512	—	—	47	18	—
Azila (25) (Malasia)	240	40.8	17	81.2	56.7	—
Keast (14) (Poland)	36	28	28	94	33	11
Keast (14) (New Zeland)	144	29	33	84	28	24
Basic (29) (Crotia)	212	21	—	—	—	10.4
Bolger (30) (USA)	202	15.7	26.1	98.5	45.1	—
Jones (31) (Ireland)	200	20	11.5	95.5	9	8
Lloyd (33) (Ireland)	100	14	17	3	2	—
Perez-Pinas (34) (Spain)	110	34	27	100	3	11
Tonai (35) (Japan)	75	28	25.3	86.7	36	—

In their study of 300 subjects, Elwany et al. [20] found a difference between the two sides of the ethmoid roof heights >3 mm in 190 cases (63.3%) (165 male, 30 female). Alazzawi et al. [12] found a height difference >2 mm between the two sides in seven (4.6%) cases. Dessi et al. [25] found a >2 mm height difference between the two sides in 13 (8.6%) cases. In our study, the difference between the heights of the right and left sides was >2 mm in 10 (2%) cases (4 female, 6 male).

A study by Reib et al. [11] is one of few that have examined ethmoid roof asymmetry. They found an asymmetrical ethmoid roof height in 221 (31%) cases. They found a lower right side ethmoid roof height in 160 (25%) cases and a lower left side ethmoid roof height in 61 (9%) cases. Reib et al. [11] also reported a higher asymmetrical ethmoid roof height in men (38%) than in women (29%). In their study, Alazzawi et al. [12] found asymmetry between the right and left LLCP heights in 139 (93%) cases. They found lower LLCP heights for the right side in 71 (51%) of these cases and a lower ethmoid height of the left side in 68 (49%) cases. In their 300-case study with 150 females and 150 males, Elwany et al. [17] found a lower average ethmoid height in women than in men. They determined that the ethmoid roof height was asymmetrical in more than 50% of the cases. They reported a statistically significant height difference between the right and left sides in women and men. In their retrospective study with 200 cases, Lebowitz et al. [26] found asymmetric ethmoid roof heights in 19 cases. They found that the right side ethmoid roof height was lower in 12 (63.2%) cases and that the left side ethmoid roof height was lower in 7 (36.6%) of the cases in which asymmetry was determined. In their study using 150 Italian patients, Dessi et al. [25] found ethmoid roof height asymmetry in 15 (10%) cases. They found a lower average right ethmoid roof height than left ethmoid roof height in 13 of the cases with asymmetry. In their study, Kızılkaya et al. [10] found a lower ethmoid roof height on the right side in 43 (25.90%) cases, a lower height on the left side in 20 (12.05%) cases and a symmetrical height in 103 cases. In their study conducted on a Turkish population, Erdem et al. [20] found ethmoid roof height asymmetry in 70 (51.5%) of their 136 cases. They did not find any significant differences in the distribution of asymmetric cases between the right and left sides. In our study, asymmetry between right and left LLCP heights was determined in 400 (80%) cases. Of the cases with asymmetry, the ethmoid roof height was lower on the right side in 216 (43.2%) cases and was lower on the left side in 184 (36.8%) cases. No differences regarding the frequency of low ethmoid roof height or in symmetry-asymmetry rates were found between females and males.

The depth from the junction of the cribriform plate and fovea ethmoidalis, as well as the configuration and symmetries of these structures are important. In a retrospective study on 200 paranasal tomographies by Lebowitz et al. [26], 86 cases were found to have a symmetrical ethmoid roof with equal heights, configuration asymmetry in 96 cases and both configuration and depth asymmetry in 1 case. In their study on 160 Chinese cases, Fan et al. [27] found ethmoid roof height asymmetry in 15.6% and fovea configuration asymmetry in 38.75% of the cases. In their study on a Turkish population, Şahin et al. [21] found ethmoid roof height asymmetry in 19 cases (19%), and fovea configuration asymmetry in 37

cases (37%). They also found configuration asymmetry in 12 (12%) of the 19 cases with height asymmetry. In the study presented here, ethmoid roof height asymmetry was found in 400 cases (80%) and fovea configuration asymmetry was found in 175 cases (35%). Ethmoid roof height asymmetry was also found in 160 (32%) of the cases with fovea configuration asymmetry. Fovea configuration asymmetry was found more on the left side than the right side. Configuration asymmetry on both the right and left sides had higher rates in men than in women. The rates of the asymmetrical LLCP heights in our study were higher than patients included in studies by Kızılkaya et al. [10] and Şahin et al. [20]. This result may be because our study was conducted using a larger sample and because measurements were performed digitally.

Knowledge of anatomic variations of paranasal sinuses is crucial for avoiding complications during the ESC and for surgery success. Surgeons should be aware of the incidence rate of paranasal sinus variations in the patients that they treat, and it is necessary to obtain detailed information for anatomic variations using preoperative CT examination. The most frequently found anatomic variation in our study was nasal septum deviation (81.8%) followed by agger nasi cell (63.8%), intralamellar air cell (45%), and concha bullosa (30%). While right anterior clinoid pneumatization was more frequently found in men, MS hypoplasis and bone septum in MS was more prevalent in women. Findings regarding the anatomic variations of paranasal sinuses according to their percentages in our country and other countries are presented in Table 8 [14, 22, 25, 29-35].

In their study on cases with chronic rhinosinusitis, Azila et al. [25] reported their most prevalent anatomic variations as Ager nasi cells (83%), Haller cells (36.7%), nasal septum deviation (53.3%), and concha bullosa (40.8%) [1]. In a retrospective study of 180 cases in Poland and New Zealand, Keast et al. [14] reported that the most prevalent anatomic variation was agger nasi cells (94%/84%), which was followed by intralamellar air cells (33%/31%) and concha bullosa (28%/29%). They did not look for the presence of septum deviation [14]. The ratios of the other variations are similar to those in our study.

Maxillary sinus hypoplasia is a rare condition. B 7% maxillary sinus hypoplasia prevalence was detected in a study by Kantarcı et al. [32] that used 512 patients from the Turkish population. Bolger et al. [30] found a 10.4% rate of unilateral maxillary sinus hypoplasia. In our study, unilateral maxillary sinus hypoplasia was observed in women (1.5%) but not in men. Bilateral maxillary sinus hypoplasia was not detected.

In conclusion, the surgeon's understanding of the anatomy of a patient's ethmoid roof and its possible variations is crucial for countering possible complication risks during surgery. This study evaluated the height, classification, and configuration of the ethmoid roof, as well as paranasal sinus variations. This study also performed a final quantitative analysis and elucidated the differences between gender and its relationship with the two sides of the ethmoid roof. In our study, males had a higher prevalence of Keros type III, which makes them more susceptible to operative complications. Therefore, extra care must be taken during surgeries on males.

Conflict of interest statement: The authors declare that they have no conflict of interest to the publication of this article.

References

1. Luong A, Marple BF. Sinus surgery: indications and techniques. Clin Rev Allergy Immunol 2006; 30: 217-22. [CrossRef]
2. Dessi P, Castro F, Triglia JM, Zanaret M, Cannoni M. Major complications of sinus surgery: a review of 1192 procedures. J Laryngol Otol 1994; 108: 212-5. [CrossRef]
3. McMains KC. Safety in endoscopic sinus surgery. Curr Opin Otolareyngol Head Neck Surg 2008; 16: 247-251. [CrossRef]
4. Ulualp SO. Complications of endoscopic sinus surgery: appropriate management of complications. Curr Opin Otolaryngol Head Neck Surg 2008; 16: 252-9. [CrossRef]
5. Stammberger HR, Kennedy DW; Anatomic Terminology Group. Paranasal sinuses: anatomic terminology and nomenclature. Ann Otol Rhinol Laryngol Suppl 1995; 167: 7-16.
6. Terrier F, Weber W, Ruefenacht D, Porcellini B. Anatomy of the ethmoid: CT, endoscopic and macroscopic. AJR Am J Roentgenol 1995; 144: 493-500. [CrossRef]
7. Kainz J, Stammberger H. The roof of the anterior ethmoid: a locus minoris resistentiae in the skull base. Laryngol Rhinol Otol (Stuttg) 1998; 67: 142-9. [CrossRef]
8. Ohnishi T, Tachibana T, Kaneko Y, Esaki S. High-risk areas in endoscopic sinus surgery and prevention of complications. Laryngoscope 1993; 103: 1181-5. [CrossRef]
9. Keros P. On the practical importance of differences in the level of the cribriform plate of the ethmoid. Laryngol Otol (Stuttg) 1965; 41: 808-13.
10. Kizilkaya E, Kantarci M, Cinar Basekim C, et al. Asymmetry of the height of the ethmoid roof in relationship to handedness. Laterality 2006; 11: 297-303. [CrossRef]
11. Reiß M, Reiß G. Height of Right and Left Ethmoid Roofs: Aspects of Laterality in 644 Patients. Int J Otolaryngol 2011; 508907.
12. Alazzawi S, Omar R, Rahmat K, Alli K. Radiological analysis of the ethmoid roof in the Malaysian population. Auris Nasus Larynx 2012; 39: 393-6. [CrossRef]
13. Beale TJ, Madani G, Morley SJ. Imaging of the paranasal sinuses and nasal cavity: normal anatomy and clinically relevant anatomical variants. Semin Ultrasound CT MR 2009; 30: 2-16. [CrossRef]
14. Keast A, Yelavich S, Dawes P, Lyons B. Anatomical variations of the paranasal sinuses in Polynesian and New Zealand European computerized tomography scans. Otolaryngol Head Neck Surg 2008; 139: 216-21. [CrossRef]
15. Stammberger H. Special endoscopic anatomy of the lateral nasal wall and ethmoidal sinuses. In: BC Decker, ed. Functional

Sinus Surgery. Philadelphia, 1991; pp.49-87.
16. Keros P. On the practical value of differences in the level of the lamina cribrosa of the ethmoid. Z Laryngol Rhinol Otol 1992; 41: 809-13.
17. Souza SA, Souza MMA, Idagawa M, Wolosker AMB, Ajzen SA. Computed tomography assessment of the ethmoid roof: a relevant region at risk in endoscopic sinus surgery. Radiol Bras 2008; 4: 143-7. **[CrossRef]**
18. Solares CA, Lee WT, Batra PS, Citardi MJ. Lateral Lamella of the cribriform plate. Software-enabled computed tomographic analysis and its clinical relevance in skull base surgery. Arch Otolaryngol Head Neck Surg 2008; 134: 285-9. **[CrossRef]**
19. Erdem G, Erdem T, Miman MC, Ozturan O. A radiological anatomic study of the cribriform plate compared with constant structures. Rhinology 2004; 42: 225-9.
20. Şahin C, Yılmaz YF, Titiz A, Özcan M, Özlügedik S, Ünal A. Analysis of Ethmoid Roof and Cranial Base in Turkish Population. KBB ve BBC Dergisi 2007; 15: 1-6.
21. Meloni F, Mini R, Rovasio S, Stomeo F, Teatini GP. Anatomic variations of surgical importance in ethmoid labyrinth and sphenoid sinus. A study of radiologic anatomy. Surg Radiol Anat 1192; 14: 65-70.
22. Arslan H, Aydınlıoglu A, Bozkurt M, Egeli E. Anatomic variations of the paranasal sinuses :CT examination for endoscopic sinus surgery. Aurius Nasus Larynx 1999; 26: 39-48. **[CrossRef]**
23. Arikan OK, Unal B, Kazkayasi M, Koc C. The analsis of anterior skull base from two different perspectives: coronal and reconstructed sagittal computed tomography. Rhinology 2005; 43: 115-20.
24. Elwany S, Medanni A, Eid M, Aly A, El-Daly A, Ammar SR. Radiological observations on the olfactory fossa and ethmoid roof. J Laryngol Otol 2010; 124: 1251-6. **[CrossRef]**
25. Azila A, Irfan M, Rohaizan Y, Shamim AK. The prevalence of anatomical variations in osteomeatal unit in patients with chronic rhinosinusitis. Med J Malaysia 2011; 66: 191-4.
26. Dessi P, Moulin G, Triglia JM, Zanaret M, Cannoni M. Difference in the height of the right and left ethmoidal roofs: a possible risk factor for ethmoidal surgery. Prospective study of 150 CT scans. J Laryngol Otol 1994; 108: 261-2. **[CrossRef]**
27. Lebowitz RA, Terk A, Jacobs JB, Holliday RA. Asymmetry of the ethmoid roof: analysis using coronal computed tomography. Laryngoscope 2001; 111: 2122-4. **[CrossRef]**
28. Fan J, Wu J, Wang H, et al. Imaging analysis of the ethmoid roof. Lin Chuang Er Bi Yan Hou Ke Za Zhi 2005; 19: 69-71.
29. Basić N, Basić V, Jukić T, Basić M, Jelić M, Hat J. Computed tomographic imaging to determine the frequency of anatomical variations in pneumatization of the ethmoid bone. Eur Arch Otorhinolaryngol 1999; 256: 69-71. **[CrossRef]**
30. Bolger WE, Woodruff WW Jr, Morehead J, Parsons DS. Maxillary sinus hypoplasia: classification and description of associated uncinate process hypoplasia. Otolaryngol Head Neck Surg 1990; 103: 759-65.
31. Jones NS, Strobl A, Holland I. A study of the CT findings in 100 patients with rhinosinusitis and 100 controls. Clin Otolaryngol 1997; 22: 47-51. **[CrossRef]**
32. Kantarci M, Karasen RM, Alper F, Onbas O, Okur A, Karaman A. Remarkable anatomic variations in paranasal sinus region and their clinical importance. Eur J Radiol 2004; 50: 296-302. **[CrossRef]**
33. Lloyd G. CT of the paranasal sinuses: study of control series in relation to endoscopic sinus surgery. J Laryngol 1990; 104: 477- 81. **[CrossRef]**
34. Pérez-Piñas, Sabaté J, Carmona A, Catalina-Herrera CJ, Jiménez-Castellanos J. Anatomical variations in the human paranasal sinus region studied by CT. J Anat 2000; 197: 221-7. **[CrossRef]**
35. Tonai A, Baba S. Anatomic variations of the bone in sinonasal CT. Acta Otolaryngol Suppl 1996; 525: 9 -13.